This article has been accepted for publication in a future issue of this journal, but has not been fully edited. Content may change prior to final publication. Citation information: DOI 10.1109/TNSE.2017.2674026, IEEE Transactions on Network Science and Engineering

A Test of Hypotheses for Random Graph Distributions Built From EEG Data

Andressa Cerqueira, Daniel Fraiman, Claudia D. Vargas and Florencia Leonardi

Abstract—The theory of random graphs has been applied in recent years to model neural interactions in the brain. While the probabilistic properties of random graphs has been extensively studied, the development of statistical inference methods for this class of objects has received less attention. In this work we propose a non-parametric test of hypotheses to test if a sample of random graphs was generated by a given probability distribution (one-sample test) or if two samples of random graphs were originated from the same probability distribution (two-sample test). We prove a Central Limit Theorem providing the asymptotic distribution of the test statistics and we propose a method to compute the quantiles of the finite sample distributions by simulation. The test makes no assumption on the specific form of the distributions and it is consistent against any alternative hypothesis that differs from the sample distribution on at least one edge-marginal. Moreover, we show that the test is a Kolmogorov-Smirnov type test, for a given distance between graphs, and we study its performance on simulated data. We apply it to compare graphs of brain functional network interactions built from electroencephalographic (EEG) data collected during the visualization of point light displays depicting human locomotion.

Index Terms—random graphs, non-parametric test of hypotheses, Kolmogorov-Smirnov test, EEG

1 Introduction

The brain consists in a complex network of interconnected regions whose functional interplay is thought to play a major role in cognitive processes [1], [2], [3]. Based on an elegant representation of nodes (vertices) and links (edges) between pairs of nodes where nodes usually represent anatomically defined brain regions while links represent functional or effective connectivity [4], random graph theory is progressively allowing to explore properties of this sophisticated network [5], [6]. Such properties have been used so far to infer, for instance, about effects of brain lesion [7], ageing [8], [9], [10] and neuropsychiatric diseases (for a recent review, see [11]).

From a theoretical point of view, the most famous model of random graphs is the Erdös-Renyi model [12], [13], where the edges of the graphs are independent and identically distributed Bernoulli random variables. Besides its simplicity, this model continues to be actively studied and new properties are being discovered (see for example [14] and references therein). A generalization of the Erdös-Renyi model that has received an increasing attention in recent years and exhibits non-zero correlations between adjacent edges is the Stochastic Block Model (SBM) [15].

Notwithstanding the crescent interest of the scientific community in the graph theory applications, the development of statistical techniques to compare sets of graphs or network data is still quite limited. Some recent works have addressed the problem of community detection in SBM [16], [17], but the testing problem has been even less developed. As far as we know, the testing problem is restricted only to the identification of differences in some one dimensional graph property [6], [18], [19]. At this point it is important to remark that the number of different graphs with v nodes grows as fast as $2^{v(v-1)/2}$ which in practice is far much larger than a typical sample size analyzed. This is the reason why the testing problem is difficult and relevant given that the graph space has no total order.

In this paper we propose a goodness-of-fit test of hypothesis for random graph distributions. The statistic is inspired in a recent work by [20] where a test of hypothesis for random trees is developed. We prove a Central Limit Theorem providing the asymptotic distribution of the test statistics and we also propose a method to compute the quantiles of the finite sample distributions by means of simulation. The test makes no assumption on the specific form of the distributions and it is consistent against any alternative hypothesis that differs from the sample distribution on at least one edge-marginal. In a simulation study we show the efficiency of the test and we compare its performance with the simultaneous testing of the edge-marginals. We also apply the test to compare graphs built from electroencephalographic (EEG) signals collected during the observation of videos depicting human locomotion.

- *A. Cerqueira and F. Leonardi are with Department of Statistics, Institute of Mathematics and Statistics, University of São Paulo, Brazil*
  E-mail: andressa@ime.usp.br and florencia@usp.br
- *D. Fraiman is with Departmento de Matemática y Ciencias, Universidad de San Andrés, and CONICET, Argentina*
  E-mail: dfraiman@udesa.edu.ar
- *C.D. Vargas is with Laboratory of Neurobiology II and Center of Research in Neuroscience and Rehabilitation, Federal University of Rio de Janeiro, Brazil*
  E-mail: cvargas@biof.ufrj.br

Manuscript received (add information)

2 Definition of the test

Let V denote a finite set of vertices, with cardinal $|V| = v$, and let $\mathbb{G}(V)$ denote the set of all simple undirected graphs over V. We identify a graph $g = (V, E)$ with the indicator function $g_{ij} = \mathbf{1}\{(i,j) \in E\}$.

Assume g is a random graph with distribution π. Denote by $\pi_{ij} = \pi(g_{ij} = 1)$ (the marginal distribution over the edge (i,j)) and let Σ denote the covariance matrix of π. Given

This article has been accepted for publication in a future issue of this journal, but has not been fully edited. Content may change prior to final publication. Citation information: DOI 10.1109/TNSE.2017.2674026, IEEE Transactions on Network Science and Engineering

another probability distribution π' defined on $\mathbb{G}(V)$, we are interested in testing the hypotheses

$$H_0 \colon \pi = \pi' \quad \text{versus} \quad H_A \colon \pi \neq \pi' \,. \tag{1}$$

Given an i.i.d sample of graphs $\mathbf{g} = (g^1, \ldots, g^n)$ with distribution π, define the function $\overline{\mathbf{g}} \colon V^2 \to [0,1]$, the empirical mean of $\mathbf{g}$, by

$$\overline{\mathbf{g}}_{ij} \;=\; \frac{1}{n} \sum_{k=1}^{n} g_{ij}^k \,.$$

Then for a known distribution π', the one-sample test statistic of the test is given by

$$W(\mathbf{g}) \;=\; \sum_{ij} \big|\, \overline{\mathbf{g}}_{ij} - \pi'_{ij} \,\big| \,. \tag{2}$$

Assuming the distribution of W under the null hypothesis is known, the result of the test (1) at the significance level α is

$$\text{Reject } H_0 \quad \text{if} \quad W(\mathbf{g}) > q_{1-\alpha} \,, \tag{3}$$

where $q_{1-\alpha}$ is the $(1-\alpha)$-quantile of the distribution of W under the null hypothesis.

In the same way, given two independent samples $\mathbf{g} = (g^1, \ldots, g^n)$ and $\mathbf{g}' = (g'^1, \ldots, g'^m)$ with distributions π and π' respectively, we define the two-sample test statistic

$$W(\mathbf{g}, \mathbf{g}') \;=\; \sum_{ij} \big|\, \overline{\mathbf{g}}_{ij} - \overline{\mathbf{g}}'_{ij} \,\big| \,. \tag{4}$$

As in the one-sample test, assuming the distribution of W under the null hypothesis is known, the result of the test (1) at the significance level α is

$$\text{Reject } H_0 \quad \text{if} \quad W(\mathbf{g}, \mathbf{g}') > q_{1-\alpha} \,, \tag{5}$$

where $q_{1-\alpha}$ is the $(1-\alpha)$-quantile of the distribution of W under the null hypothesis.

Our first theoretical result shows the asymptotic distribution of the test statistics (2) and (4). Let $\Pi = (\pi_{ij})$, $\hat{\Pi} = (\overline{\mathbf{g}}_{ij})$ and $\hat{\Pi}' = (\overline{\mathbf{g}}'_{ij})$. Then we can write $W(\mathbf{g}) = \|\hat{\Pi} - \Pi\|$ and $W(\mathbf{g}, \mathbf{g}') = \|\hat{\Pi} - \hat{\Pi}'\|$, where $\|\cdot\|$ denotes the vectorized 1-norm.

Proposition 1. *Under H_0, for the one-sample test statistic we have that*

$$\sqrt{n}\big(\hat{\Pi} - \Pi\big) \xrightarrow[n\to\infty]{D} N(0, \Sigma) \,.$$

Analogously, for the two-sample test statistic we have that

$$\sqrt{\frac{nm}{n+m}}\big(\hat{\Pi} - \hat{\Pi}'\big) \xrightarrow[n,m\to\infty]{D} N(0, \Sigma) \,.$$

Remark 1. From Proposition 1 we can deduce that the test is consistent against any alternative hypothesis π' with $\pi'_{ij} \neq \pi_{ij}$ for at least one pair ij.

Proposition 1 is of interest when the covariance matrix Σ is known a priori. In this case the quantiles in (3) and (5) can be taken from the distribution of the norm $\|\cdot\|$ of a multivariate normal random variable with mean 0 and covariance matrix Σ. In any other situation the asymptotic result is of little practical use and the quantiles can be computed by means of simulation for (3) or resampling for (5). In the sequel we show how this procedure can be implemented to estimate the quantile $q_{1-\alpha}$ in (3).

Computation of $q_{1-\alpha}$ for the one-sample test (3).

1) For $i = 1, \ldots, I$ simulate $\mathbf{g^{(i)}} = (g^{(i),1}, \ldots, g^{(i),n})$ under the null hypothesis H_0.
2) Take $q_{1-\alpha}$ as the $1-\alpha$ quantile of the empirical distribution of $W(\mathbf{g^{(1)}}), \ldots, W(\mathbf{g^{(I)}})$.

We now present the computation of $q_{1-\alpha}$ in (5) based on a resampling procedure.

Computation of $q_{1-\alpha}$ for the two-sample test (5).

1) For $i = 1, \ldots, I$ take resamples $\mathbf{g^{(i)}} = (g^{(i),1}, \ldots, g^{(i),n})$ and $\mathbf{g'^{(i)}} = (g'^{(i),1}, \ldots, g'^{(i),m})$ from the pooled sample of size $n+m$.
2) Take $q_{1-\alpha}$ as the $1-\alpha$ quantile of the empirical distribution of $W(\mathbf{g^{(1)}}, \mathbf{g'^{(1)}}), \ldots, W(\mathbf{g^{(I)}}, \mathbf{g'^{(I)}})$.

Given a distance between graphs, one can obtain different test statistics by using a Kolmogorov-Smirnov test approach. We show in the sequel that this is the case for the test statistics (2) and (4), for a particular distance that we introduce in the sequel. Given the graphs $g, g' \in \mathbb{G}(V)$ we define

$$D(g, g') = \sum_{ij} (g_{ij} - g'_{ij})^2 \,.$$

Now, given a graph $g \in \mathbb{G}(V)$ and a sample $\mathbf{g} = (g^1, \ldots, g^n)$, we denote by $\bar{D}_{\mathbf{g}}(g)$ the mean distance of graph g to the sample $\mathbf{g}$; that is

$$\bar{D}_{\mathbf{g}}(g) = \frac{1}{n} \sum_{k=1}^{n} D(g, g^k) \,.$$

Proposition 2. *For the one-sample test statistic we have that*

$$W(\mathbf{g}) \;=\; \max_{g \in \mathbb{G}(V)} \big|\bar{D}_{\mathbf{g}}(g) - \pi' D(g, \cdot)\,\big| \,, \tag{6}$$

where $\pi' D(g, \cdot)$ denotes the mean distance of graph g to a random graph with distribution π', given by

$$\pi' D(g, \cdot) = \sum_{g' \in \mathbb{G}(V)} D(g, g') \pi'(g') \,.$$

Analogously, for the two-sample test statistic we have that

$$W(\mathbf{g}, \mathbf{g}') \;=\; \max_{g \in \mathbb{G}(V)} \big|\bar{D}_{\mathbf{g}}(g) - \bar{D}_{\mathbf{g}'}(g)\,\big| \,. \tag{7}$$

The proofs of Propositions 1 and 2 are postponed to Section 5.

3 Performance on Simulated Data

In this section we present the results of a simulation study in order to evaluate the performance of the test (3). As in general the covariance structure of the distribution under the null hypothesis is unknown, we compute the quantiles of the distribution of W by the simulation procedure described in Section 2. In our first figure we show that both methods of computing the quantiles in (3) produce similar power functions.

The model we simulate is a SBM with two communities. To simulate this model, we assign to each vertex a community label 1 with probability $p \in (0,1)$ or 2 with probability

This article has been accepted for publication in a future issue of this journal, but has not been fully edited. Content may change prior to final publication. Citation information: DOI 10.1109/TNSE.2017.2674026, IEEE Transactions on Network Science and Engineering

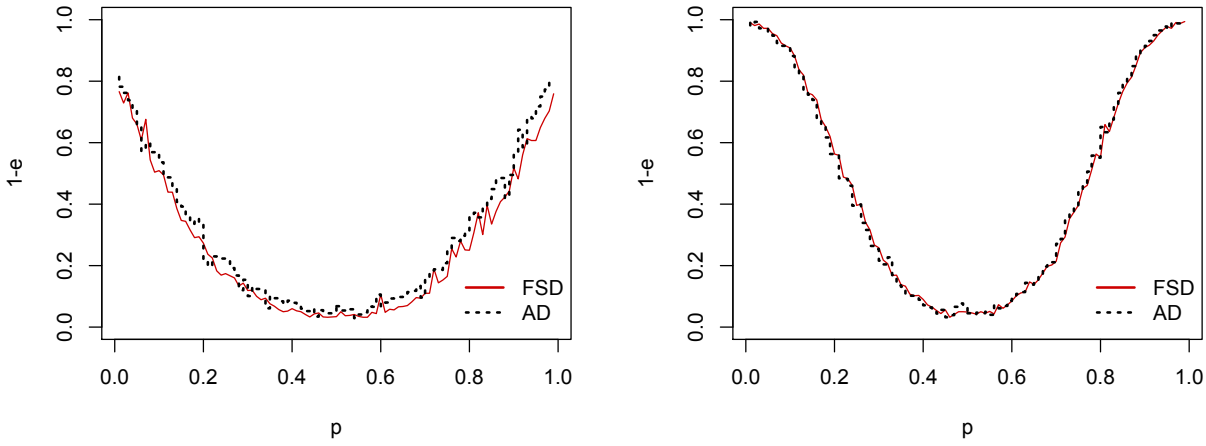

(a) $n = 10$ (b) $n = 20$

Fig. 1. Power functions of the one-sample test (3) using the quantiles from the finite sample distribution computed by simulation (FSD) and using the asymptotic distribution given in Proposition 1 (AD), for two different sample sizes. The null model is a SBM on $v = 5$ nodes with parameter $p = 0.5$ and matrix P, given by (8). The y-axis corresponds to $1 - e$, where e is the type II error of the test, computed as the proportion of times (on 1.000 replications) the test does not reject the null hypothesis when it is false, with parameter p (variable).

$1 - p$, each vertex assignment independent of any other assignment. Once the labels have been assigned, we put an edge between two edges with a probability that depends on the edges' labels, given by the matrix

$$P = \begin{pmatrix} 0.7 & 0.5 \\ 0.5 & 0.3 \end{pmatrix}. \tag{8}$$

We take as null hypothesis the SBM model with parameter $p = 0.5$ and matrix of edge probabilities P. In this case, the covariance matrix of the null distribution is given by

$$\Sigma_{ij,kl} = \begin{cases} 0, & \text{if } \{i,j\} \cap \{k,l\} = \emptyset; \\ 0.25, & \text{if } ij = kl; \\ 0.01, & \text{otherwise.} \end{cases}$$

We first show that the power function of the asymptotic test does not differ significantly from the power function obtained when the quantiles are computed by simulation, see Fig. 1. Therefore the simulation procedure shows to be efficient even for small sample sizes.

In order to compare our results with classical methods, we performed simultaneous hypothesis tests on the edge frequencies. To adjust the p-values for multiple tests, we used the method of Hommel [21] that controls the familywise error rate and the method of Benjamini-Hochberg [22] that controls the false discovery rate, see [23] for details. The (unadjusted) p-values for the set of hypotheses under the null model were obtained from the Binomial distribution with parameters $n = 20$ and $p = 0.5$, that corresponds to the marginal probability on each edge. The level of significance for the global W test was set to $\alpha = 0.05$ and for each correction method we adopted a level corresponding approximately to a global type I error α. The resulting power functions for the three approaches for different graph sizes are shown in Fig. 2.

4 Discrimination of EEG brain networks

The data analyzed in this section were first presented in [24]. A total of sixteen healthy subjects (29.25±6.3 years) with normal or corrected to normal vision and with no known neurological abnormalities participated in this study. The study was conducted in accordance with the declaration of Helsinki (1964) and approved by the local ethics committee (Comité de Ética em pesquisa do Hospital Universitário Clementino Fraga Filho, Universidade Federal do Rio de Janeiro, 303.416).

The EEG activity was recorded using a BrainNet BNT 36 (EMSA) consisting of twenty Ag/AgCl electrodes at the following scalp positions according to the 10-20 system: Fp1, Fp2, F7, F3, Fz, F4, F8, T3, C3, Cz, C4, T4, T5, P3, Pz, P4, T6, O1, Oz, O2. The impedance of each electrode was kept below 5 $k\Omega$. The electrical potential was amplified, bandpass-filtered (0.50 Hz), and digitized at a 600 Hz sampling rate, with the mastoid electrodes serving as a reference. Artifacts such as oculomotor or muscle activity were rejected offline using a threshold criterion of 50 μV, and additionally by visual inspection.

The stimulus used in the experiment is composed by 10 white luminous points with black background, that represent 10 markers of the human body (head, shoulder, elbow, hand, hip, knee and ankle). The animation of these points permitted a vivid perception of a walker's motion (which we call biological motion). The stimulus has a total length of 5200ms and is composed by 3 different phases: the visible phase (0 - 1600ms) represents the individual walking, the occlusion phase (1600ms - 3900ms) where the luminous points disappear behind a black wall and the phase of reappearance (3900ms - 5200ms) where the individual is again visible and continues walking. A second stimulus employed in that study consisted on a permuted version of the point lights, thus destroying the gestalt of the human

This article has been accepted for publication in a future issue of this journal, but has not been fully edited. Content may change prior to final publication. Citation information: DOI 10.1109/TNSE.2017.2674026, IEEE Transactions on Network Science and Engineering

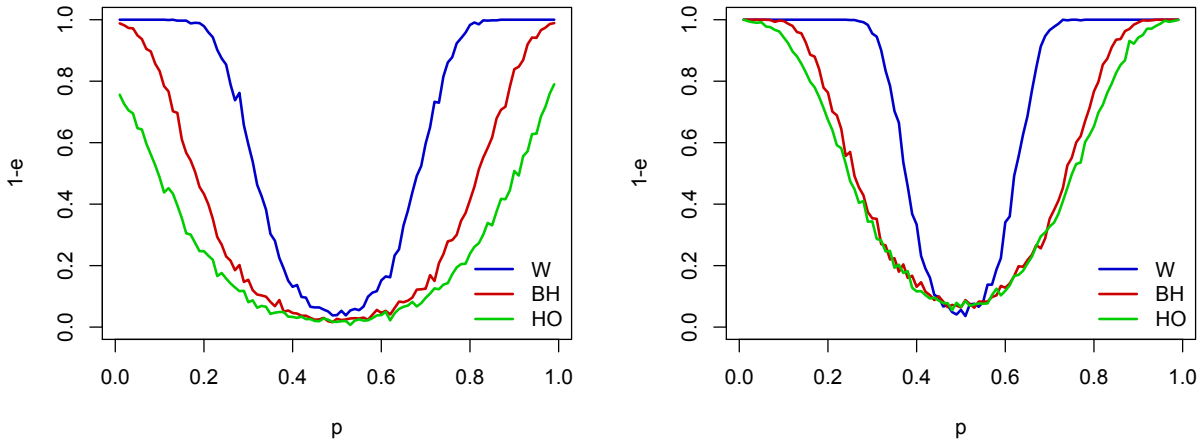

(a) $v = 10$ (b) $v = 20$

Fig. 2. Power functions of the one-sample test W and the simultaneous testing procedure with Benjamini-Hochberg (BH) and Hommel (HO) corrections. The null model is a SBM with parameter $p = 0.5$ and matrix P, given by (8), and the alternative hypothesis is a SBM with parameter p (variable) and matrix P. The sample size was fixed to $n = 20$ and the graph sizes are different for the two figures. The y-axis corresponds to $1 - e$, where e is the type II error of the test, computed as the proportion of times (on 1.000 replications) the test does not reject the null hypothesis when it is false, with parameter p.

walker motion. This stimulus is called scrambled motion. The results presented in this paper only consider the visible and the occlusion phases of the experiment (0 - 3900ms), this part of the experiment was done by seven subjects. In order to have more precise results, we partitioned both phases in four non-overlapping temporal windows of 333.3 ms (in the visible phase called V_1, V_2, V_3 and V_4 and O_1, O_2, O_3 and O_4 in the occlusion phase). A representation of the stimuli and the different time windows can be observed in the top of Fig. 3.

The experiment consisted of 25 biological motion and 25 scrambled motion stimuli presented randomly. A total of 50 point light animations were displayed (2 conditions [biological and scrambled motion, 25 repetitions). After cleaning the data we obtained 132 good trials for the visible phase and 142 for the occlusion phase of biological motion, for each temporal window (considering all subjects). In the same way, we obtained 132 trials for the visible phase and 137 trials for the occlusion phase of the scrambled motion, for each temporal window.

To construct the brain functional networks, for each subject, phase and trial of the experiment we first computed a Spearman correlation between each pair of electrodes for each temporal window $[t, t + 333ms]$, for values of t varying every 16.66ms (this corresponds to the interaction criterion in Fig. 3). The series of correlations for each pair of electrodes ij (and specific for each subject, phase and repetition) will be denoted by $\{\rho_t^{ij} : t = t_1, \ldots, t_n\}$. For the construction of the graphs we computed a threshold for each pair of electrodes ij based on this series of correlations and we put an edge between these electrodes if the absolute value of the correlation for a given time t was above this threshold (this step corresponds to the network criterion in Fig. 3). That means to say that for each pair of electrodes we selected a different threshold value, and the selection of this threshold was done in the following way. Let c be a constant, $0 < c < 1$, and let q_1^{ij} and q_3^{ij} denote the first and third quartiles of the series of correlations $\{\rho_t^{ij} : t = t_1, \ldots, t_n\}$. For a given time t define

$$g_{ij}^t = \begin{cases} 1, & \text{if } \rho_t^{ij} \geq \max(c, q_3^{ij}) \text{ or } \rho_t^{ij} \leq \min(-c, q_1^{ij}); \\ 0, & \text{otherwise} \end{cases} \tag{9}$$

In this way, the graph of interactions for time t will be given by $g^t = (g_{ij}^t)_{1 \leq i < j \leq 20}$.

The rationality of the criterion proposed here is that the graphs constructed in this way select the edges between electrodes that behaves similarly from a statistical point of view, and this is done by imposing the first and third quartile condition. Each correlation between two electrodes fluctuates in time, then for a given time t we select the ones that are too small (less than q_1^{ij}) or large (greater than q_3^{ij}). It is interpreted as follows, a given interaction grows if the two brain regions (principally responsible of the signal) are interacting in an excitatory way feeding back the process, or the interaction can decrease if there exist an inhibitory interaction between them. Both changes are captured by our criterion. The extra condition greater (or less) to the value c ($-c$) is just for obtaining statistical significant correlations. The value chosen for c in this study is 0.5.

We studied graphs at the temporal windows V1–V4 and O1–O4 that corresponds to $t = \{1.7, 335, 666.3, 1001.7\}$ (in ms) for the visual phase and $t = \{1601.7, 1935, 2268.3, 2601.6\}$ for the occlusion phase. We first tested the graphs samples corresponding to visible vs. occlusion windows; that is we tested V_1 vs. O_1, V_2 vs. O_2 and so on, for biological and scrambled motion. To compute the p-values, we used the resampling scheme

This article has been accepted for publication in a future issue of this journal, but has not been fully edited. Content may change prior to final publication. Citation information: DOI 10.1109/TNSE.2017.2674026, IEEE Transactions on Network Science and Engineering

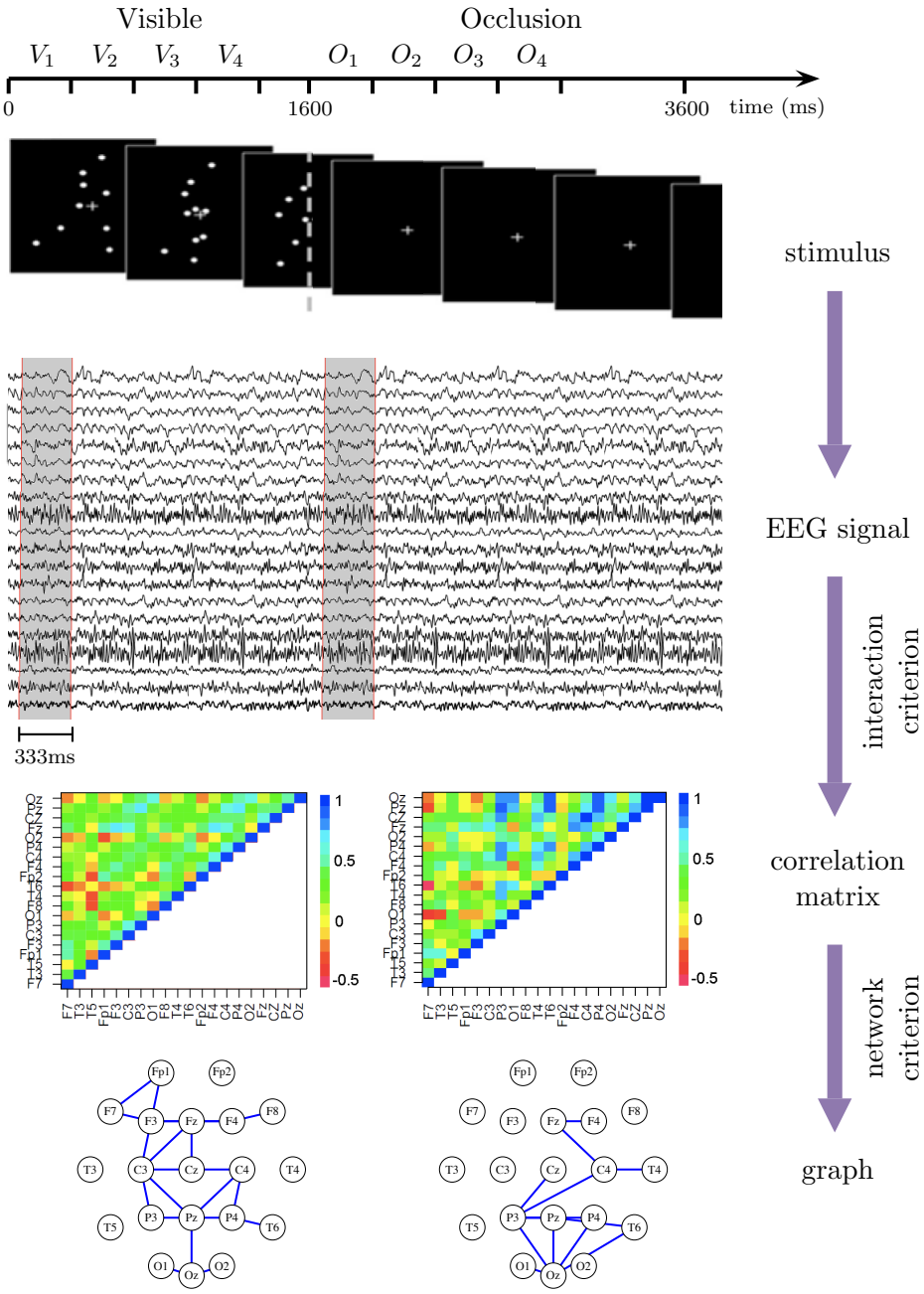

Fig. 3. First two phases of the stimulus used in the experiment and the steps to obtain the samples of graphs from the EEG signal. EEG activity was edited for simplicity.

presented in Section 2 for the two-sample W statistic, for $I = 10.000$ replications [25]. The estimated p-value is therefore the empirical proportion of values in the vector of size 10.000 built up in this way that are greater than the observed W statistic. The p-values obtained for the four tests are reported in Table 1. We notice that in both types of motion the p-values corresponding to the first windows of visible and occlusion phases are significantly smaller than the other p-values. The stimulus onset evokes an event related response [26] in the first window of the visible phase. This response, also known as visual evoked potential, is absent in the occlusion phase where there is no stimulus presentation. As can be observed the W statistic is able to retrieve this difference from the graphs distributions.

It is important to remark that the test of hypotheses proposed here does not discriminate which subgraphs in the graphs contribute more significantly to distinguish the two conditions under analysis. Therefore, to complement the results obtained with the test of hypotheses we plotted a summary graph representing each sample by selecting the 30 more frequent edges. This is a pictorial graph representation that does not reflect link dependencies that might indicate significant functional relationship between nodes. However

This article has been accepted for publication in a future issue of this journal, but has not been fully edited. Content may change prior to final publication. Citation information: DOI 10.1109/TNSE.2017.2674026, IEEE Transactions on Network Science and Engineering

Window	Biological	Scrambled
V_1 vs. O_1	**0.0019**	**0.0016**
V_2 vs. O_2	0.4294	0.8278
V_3 vs. O_3	0.1984	0.1249
V_4 vs. O_4	0.0278	0.6673

TABLE 1
P-value of the test of hypotheses for visible vs. occlusion windows of biological and scrambled motions.

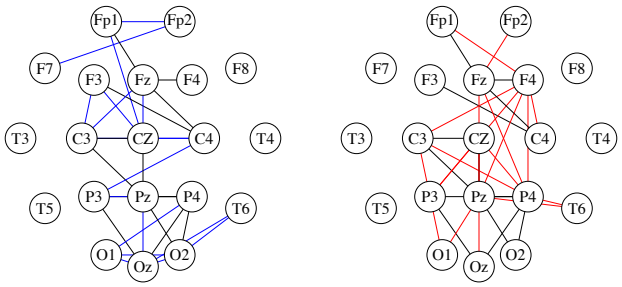

(a) Summary graphs for biological motion.

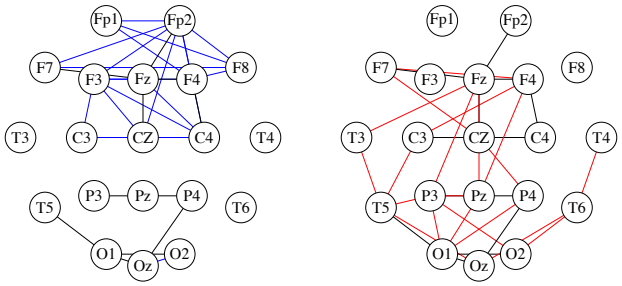

(b) Summary graphs for scrambled motion.

Fig. 4. (a) Summary graphs of 30 more frequent edges for V_1 (blue edges) and O_1 (red edges), for the biological motion. Black edges correspond to common edges. (b) Same as (a) for scrambled motion.

it represents the most frequent links thus giving relevant information on which of them are more representative in each phase.

Fig. 4(a)-(b) illustrate the graphs corresponding to V_1 and O_1 in the biological and scrambled motion conditions for which the smallest p-values were found, as illustrated in Table 1. Although the plots of the 30 most frequent edges in the first window of the visible and occlusion phases are quite similar for the biological motion condition, comparatively less edges seem present in the occipital electrodes (O1, Oz and O2) and there is a shift towards the right parietofrontal region in the occlusion period. These results could be taken as an evidence of the hypothesis raised in [24] that the brain would implicitly "reenact" the observed biological motion during the occlusion period. For the scrambled condition, the 30 most frequent edges in the first window of the visual phase clearly connect electrodes in the frontal region whereas the 30 most frequent edges in the first window of the occlusion phase connect electrodes in the central-occipital region.

These summary graphs found for biological and scrambled motions are roughly in accordance with previous reports of event related potentials (ERP) recorded from humans viewing point light display (PLD) portraying human activities. According to these studies, there is a neat tendency of such stimuli to recruit mostly the right occipito-temporal region, reflecting activity in the Superior Temporal Sulcus (STS) [24], [27], [28], [29]. This brain region is considered as an important hub at the interface between the dorsal and the ventral visual streams [30]. The participation of the parietal lobe [31], [32], [33] and the premotor cortex [34], in addition to the STS in the recognition of human motion PLD is well established. Importantly, confirming results gathered by Fraiman et al. [6] using a functional network approach, comparison of the summary graphs of biological (4a, left) and scrambled (4b, left) stimuli during the visible window clearly reveal that scrambled PLD fail to recruit the parieto-occipital network. The links during this period being concentrated in the frontal regions as compared to biological PLD activation. Interestingly, a bilateral fronto-parieto-occipital-temporal activity is reset during the occlusion phase succeeding the scrambled PLD (4b, right). The reason of such distributed network recruitment during the occlusion period that succeeds the observation of scrambled PLD is quite puzzling and deserves further investigation.

Comparing the biological and scrambled conditions during the visible phase, [24] found differences both in the right temporo-parietal and in centro-frontal regions. Using functional connectivity, [6] confirmed that the left frontal regions may play a major role when it comes to discriminating biological from scrambled motions. To confirm these findings we proceeded to test the corresponding windows of the biological and scrambled conditions. For the visible phase the smallest p-value (< 0.03) was obtained for the third temporal window (time between 668.3ms and 1001.7ms). Graph local differences have been reported in a more extended time interval form 100ms to 900ms. This interval covers mostly of the interval V3 were we found global graphs differences. It is important to remark that in [6] the authors have a larger sample size (n=16). The occlusion phase does not report significant results in any of the tested windows, see Table 2. We emphasize the fact that this is a more sensible problem compared to the comparison of visible and occlusion windows, in the sense that the differences in the stimuli are very subtle. For that reason it is not surprising that with the actual sample sizes (n=7) we do not obtain very significant results in this case.

5 Proofs

Proof of Proposition 1. This is a direct consequence of the multidimensional Central Limit Theorem (cf. Theorem 11.10 in [35]). □

Proof of Proposition 2. We will prove the proposition only for the one-sample test. The result for the two-sample test

This article has been accepted for publication in a future issue of this journal, but has not been fully edited. Content may change prior to final publication. Citation information: DOI 10.1109/TNSE.2017.2674026, IEEE Transactions on Network Science and Engineering

Window	Visible	Occlusion
1	0.1014	0.8227
2	0.6621	0.8816
3	**0.0295**	0.3764
4	0.5910	0.1292

TABLE 2
p-value of the test of hypotheses for biological vs scrambled motion of visible and occlusion phases.

can be derived analogously. Denote by $w_{\mathbf{g}}(g) = \bar{D}_{\mathbf{g}}(g) - \pi' D(g,\cdot)$. Observe that in order to maximize $|w_{\mathbf{g}}(g)|$ in $\mathbb{G}(V)$ it is sufficient to maximize $w_{\mathbf{g}}(g)$ and $-w_{\mathbf{g}}(g)$. We have that

$$w_{\mathbf{g}}(g) \;=\; \frac{1}{n}\sum_{k=1}^{n} D(g,g^k) - \sum_{g'\in\mathbb{G}(V)} D(g,g')\pi'(g')\,.$$

The first sum equals

$$\begin{aligned}\frac{1}{n}\sum_{k=1}^{n} D(g,g^k) &= \frac{1}{n}\sum_{k=1}^{n}\sum_{ij}(g_{ij}-g_{ij}^k)^2\\ &= \sum_{ij}(g_{ij} - 2g_{ij}\overline{\mathbf{g}}_{ij} + \overline{\mathbf{g}}_{ij})\,.\end{aligned}$$

The second sum is

$$\begin{aligned}\sum_{g'\in\mathbb{G}(V)} D(g,g')\pi'(g') &= \sum_{g'\in\mathbb{G}(V)}\pi'(g')\sum_{ij}(g_{ij}-g'_{ij})^2\\ &= \sum_{ij}(g_{ij} - 2g_{ij}\pi'_{ij} + \pi'_{ij})\,.\end{aligned}$$

Therefore we have that

$$w_{\mathbf{g}}(g) \;=\; \sum_{ij}(2g_{ij}-1)(\pi'_{ij} - \overline{\mathbf{g}}_{ij})\,. \tag{10}$$

As this is a weighted sum, the graph $g^* \in \mathbb{G}(V)$ that maximizes $w_{\mathbf{g}}(g)$ is given by

$$g^*_{ij} = \begin{cases}1, & \text{if } \overline{\mathbf{g}}_{ij} \le \pi'_{ij}\\ 0, & \text{otherwise}\end{cases} \tag{11}$$

Similarly, the graph $g^{**} \in \mathbb{G}(V)$ that maximizes $-w_{\mathbf{g}}(g)$ is given by

$$g^{**}_{ij} = \begin{cases}1, & \text{if } \overline{\mathbf{g}}_{ij} \ge \pi'_{ij}\\ 0, & \text{otherwise}\end{cases} \tag{12}$$

Note also that by a direct calculation from (10) and the definitions (11) and (12) we have that $|w_{\mathbf{g}}(g)| = |-w_{\mathbf{g}}(g)|$. Finally, from (6) and (11) we obtain

$$\max_{g\in\mathbb{G}(V)} |w_{\mathbf{g}}(g)| \;=\; w_{\mathbf{g}}(g^*) \;=\; \sum_{ij}|\overline{\mathbf{g}}_{ij} - \pi'_{ij}| \;=\; W(\mathbf{g})\,. \quad \square$$

6 Discussion

In this paper we presented a goodness-of-fit non-parametric test inspired in the recent work by [20] for probability distributions over graphs. To our knowledge this is the first nonparametric goodness-of-fit test of hypothesis for random graphs distributions. We show that the test statistics can be obtained from a Kolmogorov-Smirnov approach from a specific distance between graphs, and that it is consistent against any alternative hypothesis having at least one different marginal distribution over the set of edges. In this case, the simulations show that our test outperforms the simultaneous testing of the marginal means with Hommel and Benjamini-Hochberg correction methods. As in practice the sample sizes are very small compared with the sample space (in our simulations we took $n = 20$ for the sample size versus 2^{45} of the sample space for graphs with 10 nodes), our test performs very well even for small differences in the marginal distributions. In the real EEG dataset, we showed the potentiality of the W statistic to detect differences in graphs of interaction built from EEG data even for small sample sizes.

Although the main focus of this paper is on simple non-directed graphs, the generalization of the test statistic to other graph structures is possible. In particular, all the definitions and results in Section 2 are valid also for weighted graphs; that is graphs $g \in \mathbb{G}(V)$ such that $g_{ij} \in [-a, a]$, with $a \in \mathbb{R}$. On the other hand, other possible generalization of the test is to consider a different distance function between graphs or to modify the test statistic formula given in Proposition 2, taking into account the correlation structure of the set of edges. This would enable the test statistic to be consistent for different graph distributions having the same marginals over the edges, but it can not be forgotten that a modification of the test statistic can result in an increase in the computational time, which can be prohibited for large datasets.

Acknowledgments

F.L. is partially supported by a CNPq-Brazil fellowship (304836/2012-5). She also thanks L'Oréal Foundation for a "Women in Science" grant. A.C is supported by CNPq-Brazil fellowship (132940/2012-4).
This article was produced as part of the activities of FAPESP Research, Innovation and Dissemination Center for Neuromathematics, grant 2013/07699-0, São Paulo Research Foundation.

References

[1] A. Aertsen, G. Gerstein, M. Habib, and G. Palm, "Dynamics of neuronal firing correlation: modulation of" effective connectivity," Journal of neurophysiology, vol. 61, pp. 900–917, 1989.
[2] K. Friston, P. Frith, P. add Liddle, and R. Frackowiak, "Functional connectivity: the principal-component analysis of large (pet) data sets," Journal of cerebral blood flow and metabolism, vol. 13, pp. 5–14, 1993.
[3] M. Van Den Heuvel and H. Pol, "Exploring the brain network: a review on resting-state fmri functional connectivity," European Neuropsychopharmacology, vol. 8, pp. 519–534, 2010.
[4] E. Bullmore and O. Sporns, "Complex brain networks: graph theoretical analysis of structural and functional systems," Nature Reviews Neuroscience, vol. 10, no. 3, pp. 186–198, Feb. 2009. [Online]. Available: http://dx.doi.org/10.1038/nrn2575
[5] C. Calmels, M. Foutren, and C. Stam, "Beta functional connectivity modulation during the maintenance of motion information in working memory: importance of the familiarity of the visual context," Neuroscience, vol. 212, pp. 49–58, 2012.
[6] D. Fraiman, G. Saunier, E. Martins, and C. Vargas, "Biological motion coding in the brain: analysis of visually-driven eeg funcional networks," Plos One., p. 0084612, 2014.

This article has been accepted for publication in a future issue of this journal, but has not been fully edited. Content may change prior to final publication. Citation information: DOI 10.1109/TNSE.2017.2674026, IEEE Transactions on Network Science and Engineering

[7] L. Wang, C. Yu, H. Chen, W. Qin, Y. He, F. Fan, Z. W., W. M., K. Li, Y. Zang, T. Woodward, and C. Zhu, "Dynamic functional reorganization of the motor execution network after stroke," Brain, vol. 133, pp. 1224–1238, 2010.

[8] S. Achard and E. Bullmore, "Efficiency and cost of economical brain functional networks," PLoS Computational Biology, vol. 3, pp. 174–183, 2007.

[9] T. Wu, Y. Zang, L. Wang, X. Long, M. Hallett, Y. Chen, L. Kuncheng, and P. Chan, "Aging influence on functional connectivity of the motor network in the resting state," Neuroscience letters, vol. 422, pp. 164–168, 2007.

[10] D. Meunier, S. Achard, A. Morcom, and E. Bullmore, "Age-related changes in modular organization of human brain functional networks," Neuroimage, vol. 44, pp. 715–723, 2009.

[11] D. Bassett and E. Bullmore, "Human brain networks in health and disease," Current opinion in neurology, vol. 22, pp. 340–347, 2009.

[12] E. N. Gilbert, "Random graphs," Ann. Math. Statist., vol. 30, pp. 1141–1144, 1959.

[13] P. Erdős and A. Rényi, "On the evolution of random graphs," Magyar Tud. Akad. Mat. Kutató Int. Közl., vol. 5, pp. 17–61, 1960.

[14] S. Chatterjee and S. Varadhan, "The large deviation principle for the Erdős-Rényi random graph," European J. Combin., vol. 32, no. 7, pp. 1000–1017, 2011. [Online]. Available: http://dx.doi.org/10.1016/j.ejc.2011.03.014

[15] P. W. Holland, K. B. Laskey, and S. Leinhardt, "Stochastic blockmodels: first steps," Social Networks, vol. 5, no. 2, pp. 109–137, 1983. [Online]. Available: http://dx.doi.org/10.1016/0378-8733(83)90021-7

[16] A. A. Amini, A. Chen, P. J. Bickel, and E. Levina, "Pseudo-likelihood methods for community detection in large sparse networks," The Annals of Statistics, vol. 41, no. 4, pp. 2097–2122, 2013.

[17] M. E. J. Newman, "Equivalence between modularity optimization and maximum likelihood methods for community detection," Phys. Rev. E, vol. 94, p. 052315, Nov 2016. [Online]. Available: http://link.aps.org/doi/10.1103/PhysRevE.94.052315

[18] M. Boersma, D. Smit, H. de Bie, C. Van Baal, D. Boomsma, E. de Geus, H. Delemarre-van de Wall, and C. Stam, "Network analysis of resting state eeg in the developing young brain: Structure comes with maturation." Hum. Brain Mapp., vol. 32, pp. 413–425, 2011.

[19] P. Barttfeld, A. Petroni, S. Baez, H. Urquina, M. Sigman, M. Cetkovich, T. Torralva, F. Torrente, A. Lischinsky, X. Castellanos, F. Manes, and A. Ibanez, "Functional connectivity and temporal variability of brain connections in adults with attention deficit/hyperactivity disorder and bipolar disorder." Neuropsychobiology, vol. 69, pp. 65–75, 2014.

[20] J. Busch, P. Ferrari, A. Flesia, R. Fraiman, S. Grynberg, and F. Leonardi, "Testing statistical hypothesis on random trees and applications to the protein classification problem," Ann. Appl. Stat., vol. 3, no. 2, pp. 542–563, 2009. [Online]. Available: http://dx.doi.org/10.1214/08-AOAS218

[21] G. HOMMEL, "A stagewise rejective multiple test procedure based on a modified bonferroni test," Biometrika, vol. 75, no. 2, p. 383, 1988. [Online]. Available: + http://dx.doi.org/10.1093/biomet/75.2.383

[22] Y. Benjamini and Y. Hochberg, "Controlling the false discovery rate: A practical and powerful approach to multiple testing," Journal of the Royal Statistical Society. Series B (Methodological), vol. 57, no. 1, pp. 289–300, 1995.

[23] J. J. Goeman and A. Solari, "Multiple hypothesis testing in genomics," Statistics in Medicine, vol. 33, no. 11, pp. 1946–1978, 2014. [Online]. Available: http://dx.doi.org/10.1002/sim.6082

[24] G. Saunier, E. Martins, E. Dias, J. d. Oliveira, T. Pozzo, and C. Vargas, "Electrophysiological correlates of biological motion permanence in humans," Behavioural Brain Research, vol. 236, pp. 166–174, 2013.

[25] B. Manly, Randomization, bootstrap and Monte Carlo methods in biology, 3rd ed., ser. Chapman & Hall/CRC Texts in Statistical Science Series. Chapman & Hall/CRC, Boca Raton, FL, 2007.

[26] T. Picton, S. Bentin, P. Berg, E. Donchin, S. Hillyard, R. Johnson, G. Miller, W. Ritter, D. Ruchkin, M. Rugg, and M. Taylor, "Guidelines for using human event-related potentials to study cognition: Recording standards and publication criteria," Psychophysiology, vol. 37, pp. 127–152, 3 2000.

[27] M. Hirai, H. Fukushima, and K. Hiraki, "An event-related potentials study of biological motion perception in humans," Neurosci Lett, vol. 344, pp. 41–44, 2003.

[28] D. Jokisch, I. Daum, B. Suchan, and N. Troje, "Structural encoding and recognition of biological motion: evidence from event-related potentials and source analysis," Behav Brain Res, vol. 157, pp. 195–204, 2003.

[29] A. Krakowski, L. Ross, A. Snyder, P. Sehatpour, S. Kelly, and J. Foxe, "The neurophysiology of human biological motion processing: A high-density electrical mapping study," NeuroImage, vol. 56, pp. 373–383, 2011.

[30] L. Vaina and C. Gross, "Perceptual deficits in patients with impaired recognition of biological motion after temporal lobe lesions," Proc Natl Acad Sci USA, vol. 101, pp. 16 947–51, 2004.

[31] L. Battelli, P. Cavanagh, and I. Thornton, "Perception of biological motion in parietal patients," Neuropsychologia, vol. 41, pp. 1808–1816, 2003.

[32] E. Bonda, M. Petrides, D. Ostry, and A. Evans, "Specific involvement of human parietal systems and the amygdala in the perception of biological motion," J Neurosci, vol. 16, p. 37373744, 1996.

[33] L. Vaina, J. Solomon, S. Chowdhury, P. Sinha, and J. Belliveau, "Functional neuroanatomy of biological motion perception in humans," Proc Natl Acad Sci USA, vol. 98, p. 1165611661, 2001.

[34] A. Saygin, S. Wilson, D. Hagler, E. Bates, and M. Sereno, "Point-light biological motion perception activates human premotor cortex," J Neurosci, vol. 24, p. 61818, 2004.

[35] L. Breiman, Probability, ser. Classics in Applied Mathematics. Society for Industrial and Applied Mathematics (SIAM), Philadelphia, PA, 1992, vol. 7, corrected reprint of the 1968 original. [Online]. Available: http://dx.doi.org/10.1137/1.9781611971286

Andressa Cerqueira is a PhD student at University of São Paulo since 2012. As part of her PhD, she spent a year, during 2015-2016, as an invited researcher at University Paul Sabatier, in Toulouse, France. She is a member of the Center for Research, Innovation and Diffusion in Neuromathematics (NeuroMat), funded by FAPESP and her research is focused on application of stochastic process.

Daniel Fraiman received a M.Sc. degree and a Ph. D. degree both in physics from the University of Buenos Aires, Argentina, in 2000 and 2006 respectively. He become Adjoint/Associate Professor in 2006/2015 at the Department of Mathematics and Science of the University of San Andrés, Buenos Aires, Argentina. Since 2008 he is Researcher of the National Council for Scientific and Technological Research (CONICET). He is associate investigator from the Center for Research, Innovation and Diffusion in Neuromathematics (NeuroMat). His research interests include the mathematical modeling of calcium signaling, single channel modeling, complex networks, and brain dynamics.

Claudia Vargas received a PhD in Biological Sciences (Biophysics) from the Federal University of Rio de Janeiro (UFRJ) in 1997. She is since then Associate Professor at the Institute of Biophysics Carlos Chagas Filho of the UFRJ, Brazil. She also coordinates the Center of Research in Neuroscience and Rehabilitation, based at the Institute of Neurology Deolindo Couto, UFRJ. She is co-Principal Investigator at the Center for Research, Innovation and Diffusion in Neuromathematics (CEPID NeuroMat). Her research interests are the neurophysiology and plasticity of the human motor system. More recently, within Cepid NeuroMat, she has been interested in the modeling of cortical plasticity in humans.

Florencia Leonardi received a bachelor's degree in Mathematics from the University of Mar del Plata in 2002 and a PhD degree in Bioinformatics from the University of São Paulo in 2007. After a short postdoctoral period in the same institution, she became Adjoint Professor in 2008 at the Institute of Mathematics and Statistics of the University of São Paulo. During 2014- 2015 she spent a sabbatical year as a Visiting Professor at ETHZ in Switzerland, as part of the activities of the Center for Research, Innovation and Diffusion in Neuromathematics (NeuroMat), funded by FAPESP, where she is an associate investigator. Her main research interests are inference and applications of stochastic processes.